3. Preliminary Validation Efforts

3.1. Wax/Catalyst (WCD) Experiments

As indicated earlier, to develop tomographic diagnostics to measure phase volume fraction spatial distributions in opaque multiphase flows, it is important to quantify the amount of data that is needed by tomographic reconstruction algorithms and how the quality of the reconstruction is affected by the amount of data used in the reconstruction. To this end, a set of wax/catalyst disks (WCDs) were designed and fabricated.

3.1.1. WCD Description

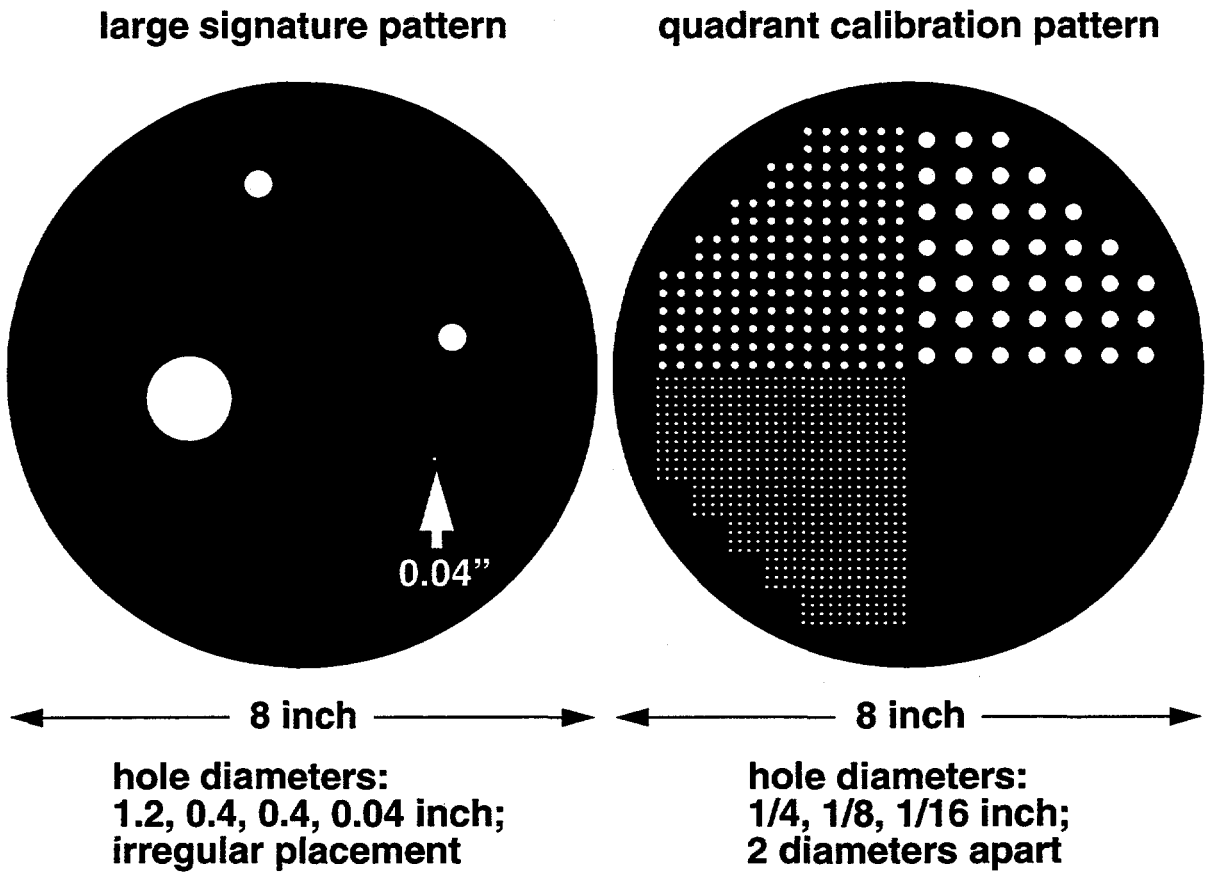

Figure 27. Wax/catalyst disk (WCD) samples with hole patterns.

Figure 27 shows the two WCDs that were fabricated. The WCDs are 20 cm (8 inches) in diameter and 5 cm (2 inches) thick. Fabrication proceeded by mixing 40% of iron-based catalyst powder by mass into molten Gulftene wax (roughly $C_{40}H_{82}$) until the powder was fairly uniformly distributed in the

wax. The mixture was then poured into molds and allowed to cool. Once solidified, the disks were removed from the molds, which was facilitated by the very slight shrinkage that occurred during cooling and solidification.

Two distinct hole patterns were bored into the disks, as shown in Figure 27. The "large signature" pattern consisted of four holes, three of which were large compared with the expected size of bubbles in the bubble column (typically a few millimeters). The "quadrant calibration" pattern consisted of one quadrant with no holes and three quadrants with the same average volume fraction occupied by the holes ($\pi/16 \approx 0.2$) with the hole diameters differing by a factor of 2 in adjacent quadrants.

3.1.2. WCD Experimental Results from XRT

To develop a GDT diagnostic technique to measure phase-volume-fraction distributions in multiphase flows, it is important to quantify the amount of data that is needed by tomographic reconstruction algorithms to accurately determine the material spatial distribution. More specifically, it is necessary to determine how the GDT reconstruction is degraded when progressively fewer projections and/or rays per projection are used for the reconstruction. Here, the terms "projection" and "ray" refer to the relative orientations of the object and a detector, respectively, with respect to the tomography system. This effect is important to quantify because one of the goals of this effort is the development of diagnostics capable of application in an industrial setting, in which it is often desirable to minimize the amount of data that must be acquired.

Since GDT and XRT employ the same physical phenomenon (attenuation of MeV-energy photons passing through the material to be examined), the previously discussed XRT facility at Sandia (Thompson and Stoker, 1997) was used to quantify the effect of the quantity of data on the quality of the tomographic reconstruction of the material distribution. Of particular interest was the minimum number of rays required to produce a reasonable reconstruction, where a single ray represents a measurement by a particular virtual detector for a particular translational position and a particular rotational position of the material to be examined. As previously indicated, since the multiphase flows ultimately to be examined by GDT are highly unsteady and spatially variable at the microscale, only macroscale information is sought (i.e. averages over a region of space that is small compared to the vessel but large compared to bubble or particle sizes). Thus, data requirements are expected to be substantially less restrictive in this application than for detailed XRT imaging of solid parts.

Three XRT data sets were obtained using the WCDs discussed in the previous section. These data sets were acquired using the following WCD configurations: the large-signature disk, the quadrant-calibration disk, and the quadrant-calibration disk surrounded with a 1.59 cm (5/8 inch) thick steel jacket fabricated by wrapping about 400 layers of 38 μm (0.0015 inch) thick sheet steel around its circumference. The purpose of the latter test was to examine the impact of a thick-walled steel vessel on the reconstruction of the material distribution within since most multiphase flows of industrial interest are contained within thick-walled vessels. Each XRT data set consisted of 360 projections of 620 rays per projection (approximately a quarter of a million data points) for a planar slice through the middle of the disk. To examine the effect of the number of rays on the quality of the tomographic reconstruction, additional data sets were created from the initial data set by systematically discarding certain rays. For the large-signature disk, entire projections were discarded: for example, every other projection was discarded to create the 180-projection data set from the original 360-projection data set. For the quadrant-calibration disk both without and with the steel jacket, 42 reduced data sets were generated from all possible combinations of 9, 18, 36, 45, 90, 180, and 360 projections with 31, 62, 124, 155, 310, and 620 rays per projection. Note that the data set (360,620), which denotes 360 projections and 620 rays per projection, is the full data set (223,200 data points)

and that the data set (9,31) is the most sparse data set (only 279 data points), so these data sets span roughly 3 orders of magnitude in amount of data.

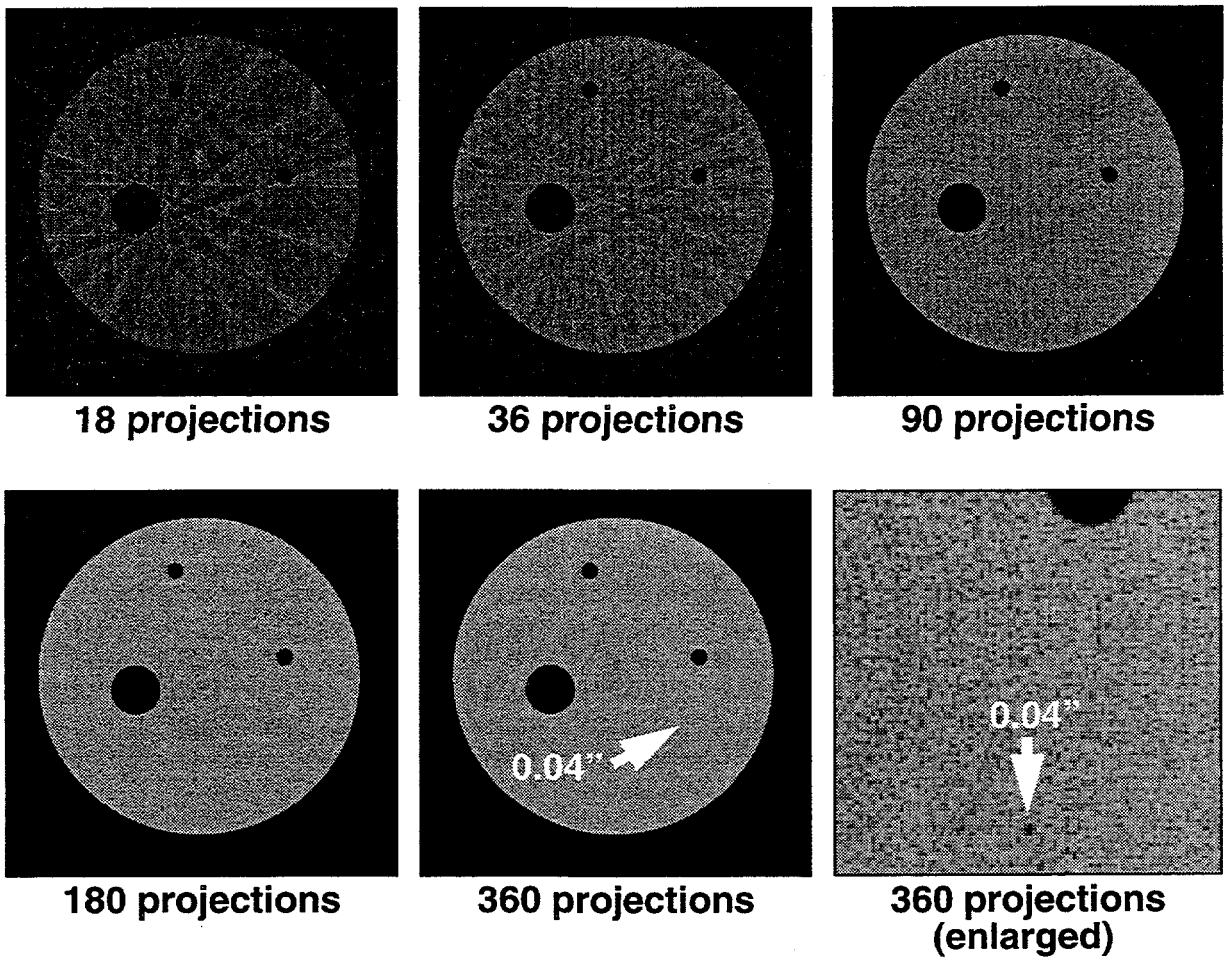

Figure 28. XRT resolution study for "large-signature" WCD.

Figure 28 shows the XRT reconstructions achieved for the large-signature WCD. Several observations can be made about these reconstructions. First, in all cases, the tomographic reconstructions are excellent. The three larger holes are accurately reproduced even with only 18 projections (i.e a factor of 20 less data than with 360 projections). However, the smallest hole is only marginally discernible for the cases with 18, 36, and 90 projections. Second, the errors produced by low resolution are streaks in the images, rather than smeared-out regions, and these streaks are always tangent to the edges of holes or the sample perimeter. Third, the amount of data used with 18 projections (11,160 points) is still rather large.

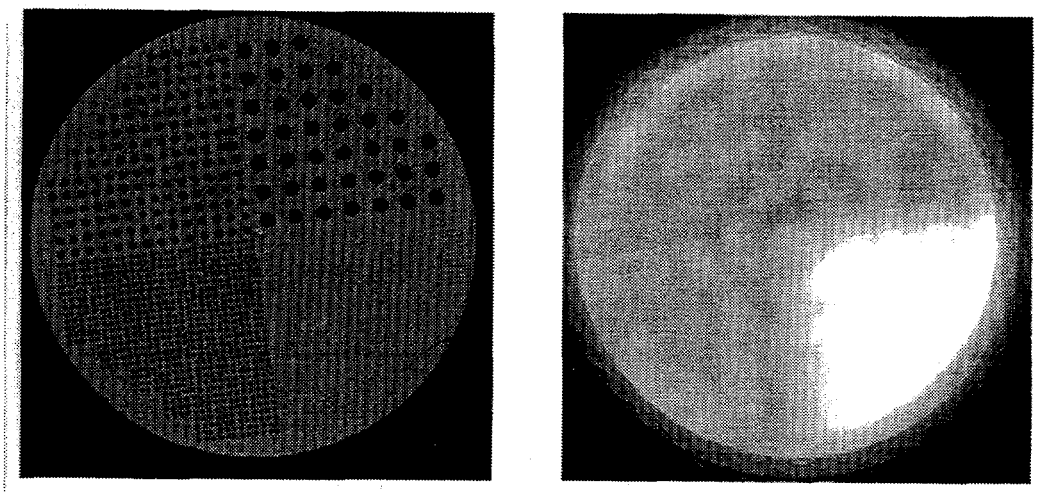

Figure 29. XRT resolution study for "quadrant calibration" WCD.

Figure 29 shows 2 of the 42 XRT reconstructions achieved for the quadrant-calibration WCD in the absence of the steel jacket. Several observations can be made about these reconstructions. First, as was true for the previous XRT experiments, the high-resolution reconstructions are excellent. The smallest diameter holes are individually visible, as are imperfections in the sample itself such as cracks near the edge and two misdrilled 1/8-inch holes. Second, the type of degradation observed in the reconstruction depends strongly on which data are discarded. Keeping the number of projections constant while reducing the number of rays per projection has the effect of gradually averaging out the data smoothly. As the number of rays per projection is decreased, the smallest holes first blur together to produce a relatively uniform background that is noticeably different from the undrilled region. Further reductions in the number of rays per projection blur out the medium holes and ultimately the large holes. Thus, reducing the number of rays per projection while fixing the number of projections acts like a spatial filter and averages out small-scale features. Keeping the number of rays per projection constant while reducing the number of projections has a rather different effect: the reconstructions become progressively more "streaky" where the streaks have the appearance of "shadows" of the holes. This was noted previously for the large-signature WCD.

Exactly the same type of XRT data set as the above was taken for the quadrant-calibration WCD with the steel jacket in place, and reduced data sets were produced in the identical manner. As was true for the previous XRT experiments, the high-resolution reconstructions were excellent. Although the steel casing clearly had a very strong signature, even the smallest diameter holes were individually visible, as were imperfections in the sample itself that were previously noted. The types of image degradation caused by reducing the number of projections or the number of rays per projection were observed to be identical to those observed in the absence of the steel jacket.

For slurry-phase bubble-column reactors, the void-fraction distribution is composed primarily of large numbers of rather small bubbles, the number density of which probably varies in a relatively smooth fashion from location to location. Thus, rather than trying to resolve very large numbers of individual bubbles, it is preferable to measure the void fraction averaged over small volumes of fluid that are

large compared to individual bubbles and inter-bubble separations but small compared to the size of the reactor and the length scale over which the bubble size distribution and number density vary appreciably. The XRT reconstructions are seen to accomplish this for the WCDs when sufficiently few rays per projection are employed so long as enough projections are used. For example, the reconstruction based on data set (36,31) is very good when judged by the standard of determining the macroscale material distribution in the sense of averaging over small volumes rather than resolving individual holes: all three drilled quadrants are clearly seen to have the same value for the average solid volume fraction, which is significantly different from the undrilled quadrant. However, using few projections with many rays does not accomplish this. Data set (9,124) possesses the same number of data points (1116) as data set (36,31), but its reconstruction (not shown but similar to those for the large-signature WCD) is much poorer in the above sense. Interestingly, the reconstruction from a "streaky" data set such as (9,124) contains information that could be used to extract hole diameters and spacings, perhaps via FFT or other standard image-processing techniques, so long as the data set was time-resolved, rather than time-averaged. This has not been investigated.

To reiterate, quite accurate XRT reconstructions of macroscopic material distribution have been produced using data sets with as few as 36 31-ray projections (1116 data points). Reconstructions based on data sets with the same number of data points but fewer projections with more rays are not as satisfactory. Thus, if restricted in the amount of data, it appears to be better to bias data collection in favor of more projections with fewer rays per projection. These observations also have ramifications for axisymmetric systems. If the field to be reconstructed is axisymmetric, only one projection is required (no new information is provided by additional projections). As a result, accurate reconstructions of fairly arbitrary axisymmetric fields can be achieved with as few as 31 rays (and possibly fewer if the field is sufficiently smooth). Thus, GDT data at roughly 30 horizontal positions is required to produce a reasonable reconstruction of the material distribution in a roughly axisymmetric system like a bubble column.

3.2. Boxed Bubble Column (BBC) Experiment

As previously discussed, the GDT system implemented herein produces inherently time-averaged data because of the long times required to collect data. However, most multiphase flows, particularly flow in a bubble column, are not steady at the microscale, and many are not steady at the macroscale for conditions of interest. Thus, some questions remain about the ability of the GDT system to produce accurate information. More specifically, if temporal variations of material distribution are large, then the use of an average intensity to determine an average attenuation coefficient will produce considerable error. This question could in principle be addressed by collecting counts for many short periods along each ray or path, determining the path-averaged attenuation for each of these periods, and temporally averaging the path-averaged attenuation (not the intensity as is currently done) prior to performing the tomographic reconstruction. Unfortunately, this is difficult to do in practice due to the large thicknesses of material to be penetrated. For example, in a bubble column, the time to collect even a few hundred counts can be comparable to hydrodynamic time scales (perhaps up to several seconds). As a result, RTR was investigated as a possible way to acquire information about temporal variations of material distribution in bubble-column flows. Of particular interest was to ascertain whether RTR could be successfully applied to observe temporal variations in the material distribution in bubble-column flows and if so to determine whether these temporal variations are large enough to invalidate using the temporally averaged intensity to calculate the temporally averaged attenuation.

3.2.1. BBC Experimental Setup

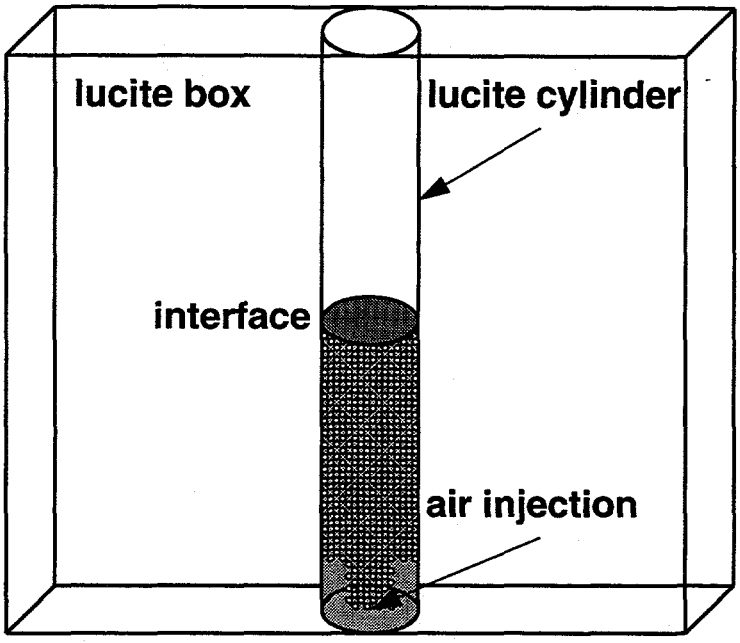

Figure 30. Boxed bubble-column experiment.

Figure 30 shows a schematic diagram of the boxed bubble-column (BBC) experiment. The column itself consisted of a lucite cylinder with an inner diameter of 10.16 cm (4 inches), a wall thickness of 0.635 cm (0.25 inches), and a height of 91.44 cm (36 inches). This cylinder was placed within a lucite box having a height equal to that of the cylinder, an inner width of 12.70 cm (5 inches), a lateral width of 43.18 cm (17 inches), and a wall thickness of 1.27 cm (0.5 inches). The purpose of the box was to allow the column to be surrounded with water to produce a region of comparable attenuation at all lateral positions relative to the cylinder axis as was thought to be necessary to produce adequate contrast. However, as it turned out, images recorded with the box filled with water did not seem to be of better contrast than those recorded with the box empty, and the latter were more visually instructive.

The BBC was typically operated as follows. The column was filled with water to a height of 60.96 cm (24 inches), and air was injected from a single tubular nozzle with inner and outer diameters of 0.79 mm and 1.57 mm centered at the bottom of the column. Air flow was produced by a small compressor attached to the orifice by a length of tubing. Adjusting the compressor pressure controlled the air flow rate, with higher pressures corresponding to higher flow rates. Unfortunately, it was not possible to quantify the relationship between the compressor pressure and the resulting volumetric flow rate of the air that resulted.

3.2.2. BBC Experimental Results from RTR

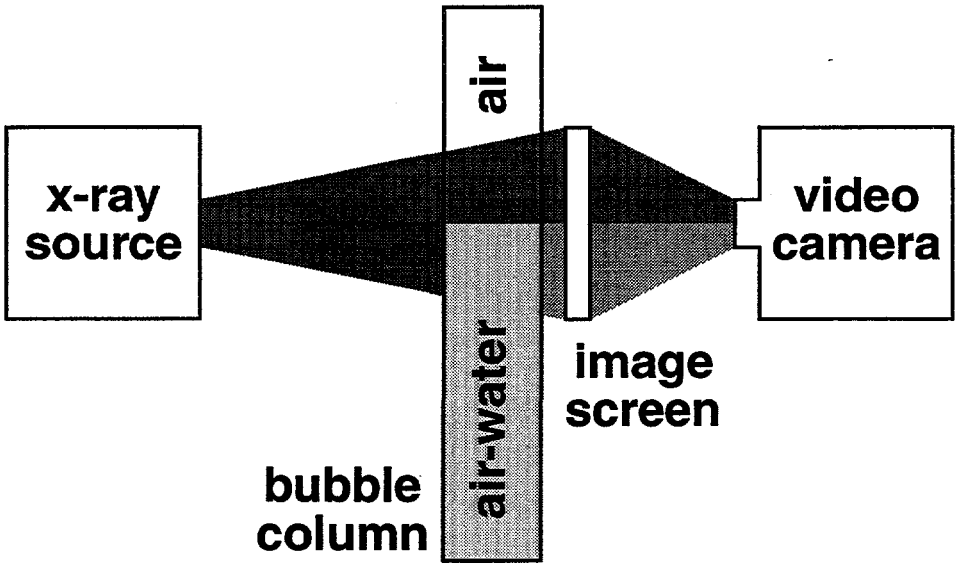

Figure 31. Schematic diagram of RTR applied to BBC experiment.

Figure 31 shows a schematic diagram of the previously described RTR system applied to the BBC experiment. The BBC was filled with water to a height of 60.96 cm (24 inches) prior to the tests and was positioned such that the undisturbed air-water interface lay just below the center of the field of view for the XRT system. Air flow was initiated and held constant while video recording were made at the standard video frame rate for a long period of time. The video results were analyzed following the tests using image-processing software. Tests were performed for several air flow rates and for the box filled with water and empty.

Figure 32 shows images recorded with the box empty for three sets of air flow rates: no air flow; slow air flow, and fast air flow. These images were produced by averaging large numbers of images for each air flow rate. Several features are apparent from these images. The time-averaged interface is observed to thicken with increasing air flow rate (the undisturbed interface position is indicated in each image). This corresponds to the visual observation that the gas-liquid interface becomes more agitated with increasing air flow rate. Also, interface midpoint is seen to be higher and the attenuation in the region below the interface is seen to decrease with increasing air flow, as would be expected since the amount of gas present in the multiphase mixture increases with the air flow rate. From comparing a few individual frames to the average images, temporal variations did not appear to be large except in the vicinity of the gas-liquid interface. However, extensive analysis of many more frames using the available image-processing software is required to confirm and quantify this conclusion. The attenuations observed with this small-diameter bubble column suggest that application of this RTR system to large-diameter bubble-column vessels with steel walls is unlikely to produce satisfactory results.

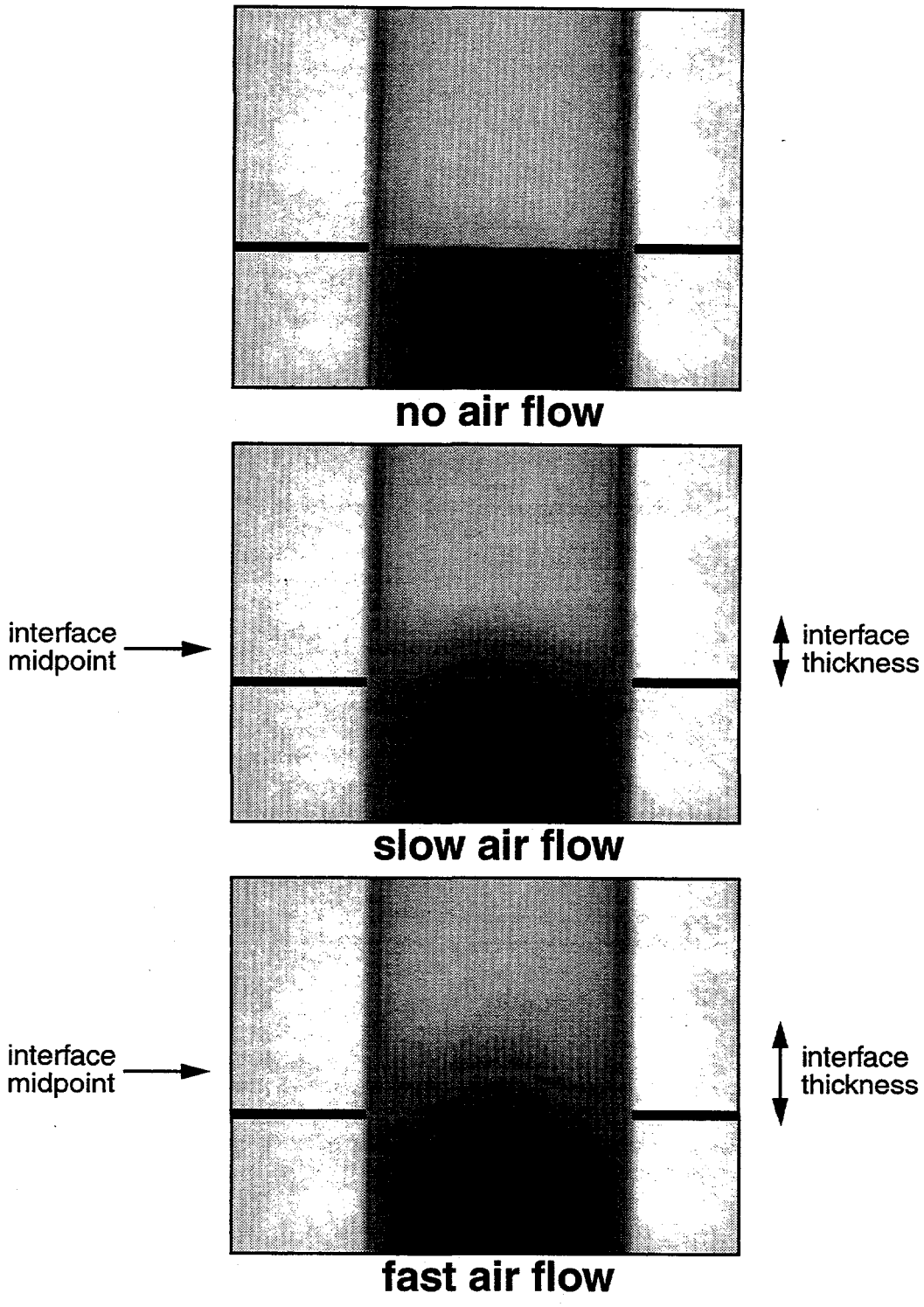

Figure 32. RTR results for BBC experiment.